

## Novel 2-Mercaptopyridine–Ruthenium Complex Exhibiting Electrochemically Induced Linkage Isomerization Switched On/Off by Protolysis

Tomohiko Hamaguchi,\* Kikujiro Ujimoto, and Isao Ando

Department of Chemistry, Faculty of Science, Fukuoka University, 8-19-1 Nanakuma, Jonan-ku, Fukuoka 814-0180, Japan

Received June 18, 2007

A ruthenium complex [ruthenium bis(2,2'-bipyridine)(2-mercaptopyridine)(pyridine)](PF<sub>6</sub>)<sub>2</sub> was crystallographically characterized from its deprotonated form and was electrochemically investigated. In the deprotonated complex, the 2-mercaptopyridine ligand coordinates to the Ru atom only by the S atom; therefore, the N atom of the 2-mercaptopyridine ligand can be protonated. In a CH<sub>3</sub>CN solution, the complex shows a reversible redox couple attributed to Ru<sup>II/III</sup>–S. The addition of a base to the CH<sub>3</sub>CN solution of the complex gives irreversible voltammograms, implying electrochemically induced linkage isomerization between Ru<sup>II</sup>–S and Ru<sup>III</sup>–N. Analysis of the observed cyclic voltammograms gave the equilibrium and rate constants for linkage isomerization:  $K^{\text{I}_{\text{NS}}} = 1.2 \times 10^{18}$ ,  $K^{\text{II}_{\text{NS}}} = 0.64$ ,  $k^{\text{I}_{\text{NS}}} = 5 \times 10 \text{ s}^{-1}$ ,  $k^{\text{I}_{\text{SN}}} = 4 \times 10^{-17} \text{ s}^{-1}$ ,  $k^{\text{II}_{\text{NS}}} = 0.26 \text{ s}^{-1}$ , and  $k^{\text{II}_{\text{SN}}} = 0.40 \text{ s}^{-1}$ .

Molecular devices,<sup>1,2</sup> especially molecular memory,<sup>2</sup> which is interesting as an advanced information storage device, have received a lot of attention. Molecular memory is able to store information into one molecule and should help in increasing the storage density. Such devices require molecular bistability, i.e., a molecule with two or more stable states that are reversibly exchanged by external stimuli. Transition-metal complexes exhibiting electrochemically induced linkage isomerization have been reported<sup>3</sup> as model compounds for molecular memory. They contain an ambidentate ligand bound to a metal center and exhibit exchange of the coordination atom for another atom on applying voltage sufficient to oxidize or reduce the metal center. A different coordination environment produces different properties of the complex; therefore, those complexes are able to *write* and *read*

information. This is an important feature for memory devices. *Write* denotes recording information by oxidation or reduction of the metal center and retaining the information as the difference in the coordination environment. *Read* denotes getting the information back from the complex as the difference in a property, e.g., UV–vis absorption.

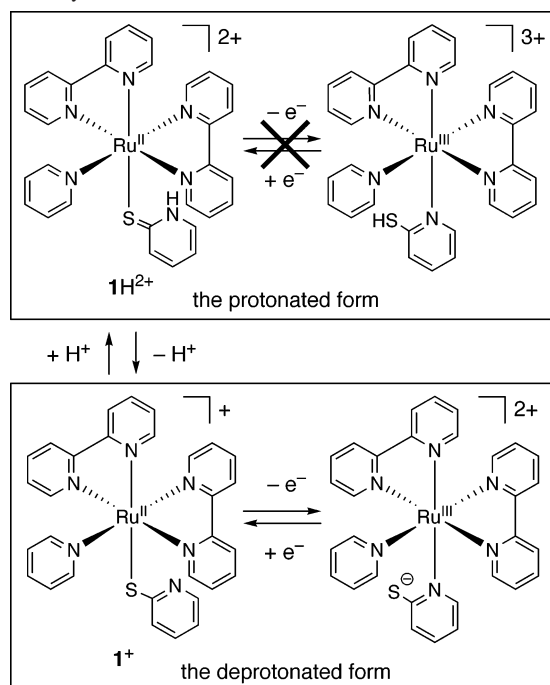
For example, [Ru<sup>II</sup>(NH<sub>3</sub>)<sub>5</sub>(DMSO)]<sup>2+</sup> (DMSO = dimethyl sulfoxide) is one of the most famous molecules exhibiting electrochemically induced linkage isomerization.<sup>4</sup> In this complex, Ru<sup>II</sup> is coordinated by the S atom of DMSO. After oxidation of Ru<sup>II</sup> to Ru<sup>III</sup>, the complex isomerizes to the other isomer in which Ru<sup>III</sup> is coordinated by the O atom. The related complexes<sup>5,6</sup> are suitable as candidates for a molecular memory device. However, they have a problem; information could be overwritten by an unintended external signal because they have no mechanism to protect information like the write-protect tab of a floppy disk. Some carboxamide-ruthenium complexes<sup>6</sup> could solve this problem, but only a few such complexes have been reported so far.<sup>5g</sup>

Here, we report a new ruthenium complex, **1H**<sup>2+</sup>, that has a mechanism to protect information. **1H**<sup>2+</sup> is designed to contain a Ru<sup>II</sup> atom and 2-mercaptopyridine in thione form,<sup>7</sup> which coordinates to the Ru atom only with the S atom. The N atom of 2-mercaptopyridine is protonated and does not coordinate to the Ru atom. Linkage isomerization from S- to N-bound is difficult in oxidation of **1H**<sup>2+</sup> because protonation of 2-mercaptopyridine prevents the N atom from

\* To whom correspondence should be addressed. E-mail: thama@fukuoka-u.ac.jp.

- (1) (a) Gunaratne, H. Q. N.; Silva, A. P.; Gunnlaugsson, T.; Huxley, A. J. M.; McCoy, C. P.; Rademacher, J. T.; Rice, T. E. *Chem. Rev.* **1997**, *97*, 1515. (b) Licchelli, M.; Pallavicini, P.; Fabbri, L. *Acc. Chem. Res.* **1999**, *32*, 846. (c) Ward, M. D. *Chem. Soc. Rev.* **1995**, *24*, 121.
- (2) (a) Carroll, R. L.; Gorman, C. B. *Angew. Chem., Int. Ed.* **2002**, *41*, 4378. (b) Fabbri, L.; Pallavicini, P.; Amendola, V. *Coord. Chem. Rev.* **2001**, *216*–217, 435.
- (3) Toma, H. E.; Rocha, R. C. *Croat. Chem. Acta* **2001**, *74*, 499.

- (4) Scotto, N.; Yen, A.; Taube, H. *Inorg. Chem.* **1982**, *21*, 2542.
- (5) (a) Giesbrecht, E.; Rojas, R. L. E.; Toma, H. E. *J. Chem. Soc., Dalton Trans.* **1985**, 2469. (b) Johansson, O.; Lomoth, R. *Chem. Commun.* **2005**, 1578. (c) Tomita, A.; Sano, M. *Inorg. Chem.* **1994**, *33*, 5825. (d) Tomita, A.; Sano, M. *Inorg. Chem.* **2000**, *39*, 200. (e) Sano, M.; Taube, H. *Inorg. Chem.* **1994**, *33*, 705. (f) Silva, D. O.; Toma, H. E. *Can. J. Chem.* **1994**, *72*, 1705. (g) Sens, C.; Rodríguez, M.; Romero, I.; Llobet, A.; Parella, T.; Sullivan, B. P.; Buchholz, J. B. *Inorg. Chem.* **2003**, *42*, 2040.
- (6) (a) Fairlie, D. P.; Ilan, Y.; Taube, H. *Inorg. Chem.* **1997**, *36*, 1029. (b) Chou, M. H.; Brunshwing, B. S.; Creutz, C.; Sutin, N.; Yeh, A.; Chang, R. C.; Lin, C.-T. *Inorg. Chem.* **1992**, *31*, 5347.
- (7) (a) Bajaj, H. C.; Das, A.; van Eldik, R. J. *J. Chem. Soc., Dalton Trans.* **1998**, 1563. (b) Deeming, A. J.; Hardcastle, K. I.; Meah, M. N.; Bates, P. A.; Dawes, H. M.; Hursthouse, M. B. *J. Chem. Soc., Dalton Trans.* **1988**, 227.

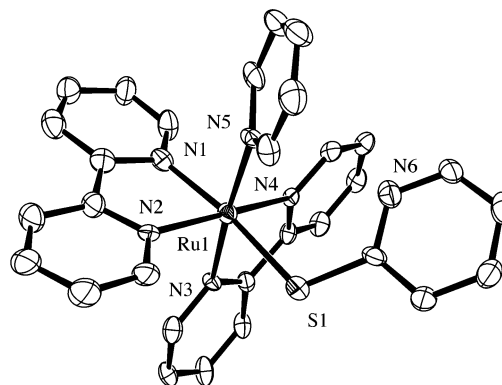
**Scheme 1.** Electrochemically Induced Linkage Isomerization Controlled by the Addition of a Base and an Acid

coordinating to the Ru atom. On the other hand, linkage isomerization may proceed upon oxidation of  $1^+$  (deprotonated form). Therefore, adding a base or an acid to the solution of the complex should control electrochemically induced linkage isomerization of  $1\text{H}^{2+}$  (Scheme 1).

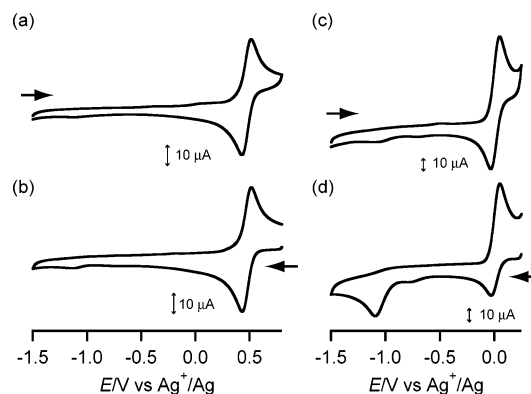
$1\text{H}^{2+}$  was prepared as a  $\text{PF}_6$  salt and was characterized by elemental analysis,  $^1\text{H}$  NMR, and UV–vis absorption. We could not obtain a suitable crystal of  $1\text{H}^{2+}$  for single-crystal X-ray analysis as a  $\text{PF}_6$  salt; however, we prepared a good crystal of the deprotonated form ( $1\cdot\text{BPh}_4$ ) by recrystallization in the presence of  $\text{NaBPh}_4$  and  $\text{Et}_3\text{N}$ .<sup>8</sup>

The ORTEP drawing of a  $1^+$  cation reveals that 2-mercaptopyridine coordinates to the Ru atom with the S atom monodentately (Figure 1). These data indicate that  $1\text{H}^{2+}$  has the intended structure that we require. The UV–vis absorption spectrum of  $1\text{H}\cdot(\text{PF}_6)_2$  in  $\text{CH}_3\text{CN}$  showed three absorption bands at 293, 354 (sh), and 454 nm. The first band is assigned to a ligand-centered  $\pi-\pi^*$  transition; the others are assigned to metal-to-ligand charge-transfer transitions. Upon the addition of  $\text{Et}_3\text{N}$  as a base, the spectrum changed with a set of isosbestic points at 335, 399, and 490 nm (Figure S1a in the Supporting Information). This change was completed with the addition of 1 equiv of a base. The initial spectrum was recovered completely upon the addition of excess  $\text{CF}_3\text{COOH}$  as an acid (Figure S1b in the Supporting Information). This confirms the reversible protolysis of  $1\text{H}^{2+}$ .

(8) Crystal data for  $1\cdot\text{BPh}_4$ :  $\text{C}_{54}\text{H}_{45}\text{BN}_6\text{RuS}$ ,  $M = 921.90$ , monoclinic,  $C2/c$ ,  $a = 33.696(10)$  Å,  $b = 9.513(3)$  Å,  $c = 30.793(8)$  Å,  $\beta = 115.828(4)^\circ$ ,  $V = 8885(4)$  Å<sup>3</sup>,  $Z = 8$ ,  $T = 100$  K, 11 939 collected reflections and 5397 independent reflections,  $R1 = 0.0675$  and  $wR2 = 0.0891$  for  $I > 2\sigma(I)$ . The structure was determined in *SHELXS-97* and refined using *SHELXL-97*.<sup>12</sup> Selected bond distances: Ru1–S1 2.396(3) Å, Ru1–N1 2.056(8) Å, Ru1–N2 2.063(7) Å, Ru1–N3 2.032(7) Å, Ru1–N4 2.056(7) Å, Ru1–N5 2.098(8) Å. Selected bond angles: N1–Ru1–S1 173.0(2)°, N3–Ru1–N5 175.7(3)°, N4–Ru1–N2 171.3(3)°.



**Figure 1.** Molecular structure of the complex cation of  $1^+$ . Thermal ellipsoids are drawn at the 50% probability level, and H atoms are omitted.

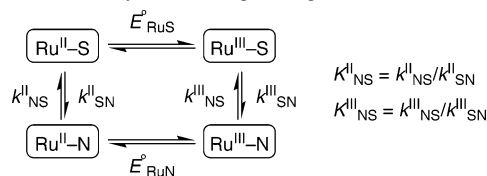


**Figure 2.** Cyclic voltammograms of  $1\text{H}^+(\text{PF}_6)_2$  in  $\text{CH}_3\text{CN}$  (a and b) and in  $\text{Et}_3\text{N}/\text{CH}_3\text{CN}$  (c and d). (a and c) Anodic scan starting at  $-1.50$  V vs  $\text{Ag}^+/\text{Ag}$ . (b and d) Cathodic scan starting at  $0.80$  and  $0.25$  V vs  $\text{Ag}^+/\text{Ag}$  after oxidation at  $0.80$  and  $0.25$  V vs  $\text{Ag}^+/\text{Ag}$  for 3 min, respectively. The arrow shows the initial scan direction. The scan rate is  $0.1$  V  $\text{s}^{-1}$ .

Cyclic voltammograms of  $1\text{H}^{2+}$  were examined in the absence and presence of  $\text{Et}_3\text{N}$  (Figures 2 and 2S in the Supporting Information).<sup>9</sup> In the absence of  $\text{Et}_3\text{N}$ , the cyclic voltammograms exhibited one reversible redox couple, associated with  $\text{Ru}^{\text{III/II}}$  at  $E_{1/2} = 0.47$  V vs  $\text{Ag}^+/\text{Ag}$  (Figure 2a,b). The shape of the voltammogram was independent of the scan direction and scan rate. These results imply that the linkage isomerization occurs sparingly during the redox reaction.

In the presence of  $\text{Et}_3\text{N}$ , the voltammograms dramatically changed depending on the scan direction and scan rate. With the anodic scan starting at  $-1.50$  V vs  $\text{Ag}^+/\text{Ag}$  (Figure 2c), one quasi-reversible redox couple, associated with  $\text{Ru}^{\text{III/II}}$  at  $E_{1/2} = 0.01$  V vs  $\text{Ag}^+/\text{Ag}$ , was observed. A small cathodic peak was observed at about  $-1$  V vs  $\text{Ag}^+/\text{Ag}$ . After oxidation at  $0.25$  V for 3 min (Figure 2d), two quasi-reversible redox couples ( $E_{1/2} = 0.01$  and  $E_{2/2} = -1.07$  V vs  $\text{Ag}^+/\text{Ag}$ ) were observed with the cathodic scan starting at  $0.25$  V vs  $\text{Ag}^+/\text{Ag}$ . The ratios of  $i_{c1}/i_{a1}$  and  $i_{c2}/i_{a2}$  were dependent on the scan rate ( $i_{c1}$  and  $i_{c2}$  are cathodic peak currents and  $i_{a1}$

(9) Cyclic voltammetry was performed on BAS100B/W (BAS) using three electrode cells (glassy carbon as the working electrode, Pt coil as the counter electrode, homemade  $\text{Ag}^+/\text{Ag}$  as the reference electrode). The medium was  $0.1$  mol  $\text{dm}^{-3}$   $n\text{-Bu}_4\text{NPF}_6/\text{CH}_3\text{CN}$  or  $1 \times 10^{-3}$  mol  $\text{dm}^{-3}$   $\text{Et}_3\text{N}/0.1$  mol  $\text{dm}^{-3}$   $n\text{-Bu}_4\text{NPF}_6/\text{CH}_3\text{CN}$ . The concentration of the complex was  $1 \times 10^{-3}$  mol  $\text{dm}^{-3}$ .  $E_{1/2}$  of the ferrocenium/ferrocene couple was  $0.10$  V vs  $\text{Ag}^+/\text{Ag}$ .

**Scheme 2.** Redox Cycle Including Linkage Isomerization

and  $i_{a2}$  are anodic peak currents at the redox peak potentials of  $E^{1/2}$  and  $E^{2/2}$ , respectively). This dramatic change suggests that electrochemically induced linkage isomerization occurs between Ru–S and Ru–N linkage isomers in  $\mathbf{1}^+$ . By analogy to the literature,<sup>5f,g</sup> the redox couples at  $E^{1/2}$  and  $E^{2/2}$  are assigned to Ru<sup>III/II</sup>–S and Ru<sup>III/II</sup>–N, respectively. The difference in voltammetric behaviors in the absence and presence of Et<sub>3</sub>N reveals that only the deprotonated form of the complex shows linkage isomerization.

To confirm this isomerization, the spectrum of the electrolytic product of  $\mathbf{1}^+$  was measured by spectroelectrochemistry (Figure S3 in the Supporting Information). The spectrum of  $\mathbf{1}^+$  did not change upon application of a potential of  $-0.3$  V vs Ag<sup>+</sup>/Ag. Upon oxidation at  $+0.35$  V, bands around 350, 500, and 600 nm disappeared, and a new band appeared around 430 nm. When the oxidized complex was reduced at  $-0.30$  V, the spectrum was almost the same as that at  $+0.35$  V rather than that at the initial  $-0.30$  V. This irreversibility might show that the complex was decomposed upon oxidation; however, the spectrum upon successive reduction at  $-1.35$  V was almost the same as that at the initial  $-0.30$  V. This shows that the complex recovered the isolated state upon reduction. When the potential was held at  $-0.30$  V, the complex retained the same spectrum. The observed hysteresis seems to suggest that  $\mathbf{1}^+$  isomerizes to Ru<sup>III</sup>–N upon oxidation and recovers Ru<sup>II</sup>–S upon reduction.

The reversibility of  $\mathbf{1H}^{2+}$  for deprotonation was also confirmed by cyclic voltammetry. As mentioned above,  $\mathbf{1H}^{2+}$  did not isomerize in CH<sub>3</sub>CN, but it did after the addition of 1 equiv of Et<sub>3</sub>N. When excess CF<sub>3</sub>COOH was added into the basic solution, this complex did not isomerize again. This shows that electrochemically induced linkage isomerization can be controlled reversibly by the addition of a base or an acid.

Scheme 2 shows the redox cycle including linkage isomerization. The equilibrium constants ( $K^{\text{II}_{\text{NS}}}$  and  $K^{\text{III}_{\text{NS}}}$ ) and rate constants ( $k^{\text{II}_{\text{NS}}}$  and  $k^{\text{III}_{\text{SN}}}$ ) for linkage isomerization were estimated from the cyclic voltammograms as follows.<sup>5f,g</sup> The value of  $K^{\text{III}_{\text{NS}}}$  can be obtained from the intercept of the plot of  $i_{c1}/i_{c2}$  against the reciprocal of the scan rates,  $v^{-1}$ . The obtained value of  $K^{\text{III}_{\text{NS}}}$  is  $0.64 \pm 0.03$  s<sup>-1</sup>. The values

of  $k^{\text{III}_{\text{NS}}}$  and  $k^{\text{III}_{\text{SN}}}$  were also evaluated from the equation for the chemical reaction preceding a reversible charge transfer (case III) proposed by Nicholson and Shain.<sup>10</sup> Assuming that  $i_k$  (the measured peak current) is  $i_{c1}$  of the voltammogram in which the initial scan direction is cathodic and  $i_d$  (the corresponding diffusion-controlled current in the absence of a chemical reaction) is  $i_{a1}$  of the voltammogram in which the initial scan direction is anodic, the evaluated values are  $k^{\text{III}_{\text{NS}}} = 0.26$  s<sup>-1</sup> and  $k^{\text{III}_{\text{SN}}} = 0.40$  s<sup>-1</sup>. The thermodynamic cycle in Scheme 2 can be solved to obtain the equilibrium constant  $K^{\text{II}_{\text{NS}}}$  for the Ru<sup>II</sup>–N/Ru<sup>II</sup>–S reaction, based on  $K^{\text{III}_{\text{NS}}}$  and assuming  $E^\circ = E^{1/2}$ . In this way,  $K^{\text{II}_{\text{NS}}} = 1.2 \times 10^{18}$ . The rate constants of  $k^{\text{II}_{\text{NS}}}$  and  $k^{\text{II}_{\text{SN}}}$  are evaluated from the simulation of the cyclic voltammograms (Figure S4 in the Supporting Information).<sup>11</sup> Because  $k^{\text{II}_{\text{SN}}}$  is dependent on  $k^{\text{II}_{\text{NS}}}$ , simulation of the cyclic voltammogram was performed upon fixing  $E^{1/2}$ ,  $E^{2/2}$ ,  $K^{\text{III}_{\text{NS}}}$ ,  $k^{\text{III}_{\text{NS}}}$ ,  $k^{\text{III}_{\text{SN}}}$ , and  $K^{\text{II}_{\text{NS}}}$  to the evaluated values and changing  $k^{\text{II}_{\text{NS}}}$  as the only variable parameter. From this simulation, we obtain  $k^{\text{II}_{\text{NS}}} = 5 \times 10$  s<sup>-1</sup> and  $k^{\text{II}_{\text{SN}}} = 4 \times 10^{-17}$  s<sup>-1</sup>.  $K^{\text{II}_{\text{NS}}}$  and  $K^{\text{III}_{\text{NS}}}$  suggest that Ru<sup>II</sup> favors hugely the S-bound isomer and Ru<sup>III</sup> does slightly favor the N-bound isomer.

In this study, we demonstrated that the complex  $\mathbf{1}^+$  shows linkage isomerization induced by the redox reaction from the S-bound form to the N-bound form. However, the protonated complex  $\mathbf{1H}^{2+}$  does not isomerize upon oxidation. Thus, the present complex can be set to forbid or allow isomerization by changing the pH of the solution and should be a candidate for molecular memory equipped with a write-protect tab.

**Acknowledgment.** The authors thank Shinetsu Igarashi and Dr. Kenji Yoza (Bruker AXS K.K.) for the X-ray crystal structure determination. This work was supported in part by funds (Grant 075001) from the Central Research Institute of Fukuoka University.

**Supporting Information Available:** Synthesis of  $\mathbf{1H} \cdot (\text{PF}_6)_2$ , absorption spectra of  $\mathbf{1H} \cdot (\text{PF}_6)_2$  upon the continuous addition of Et<sub>3</sub>N and  $\mathbf{1}^+$  upon the continuous addition of CF<sub>3</sub>COOH, cyclic voltammograms, absorption spectra of oxidized and reduced  $\mathbf{1H} \cdot (\text{PF}_6)_2$  upon the addition of 1 equiv of Et<sub>3</sub>N, and crystallographic details in CIF format. This material is available free of charge via the Internet at <http://pubs.acs.org>.

IC701186K

(10) Nicholson, R. S.; Shain, I. *Anal. Chem.* **1964**, *36*, 706.

(11) Digital simulation of proposed electrochemical mechanisms was performed with DigiSim (BAS).

(12) Sheldrick, G. M. *SHELXL-97*; University of Göttingen: Göttingen, Germany, 1997.